DETECTION AND CLASSIFICATION OF DEFECTS IN SOLAR PANEL CELLS USING DEEP LEARNING MODEL

Ogbuikwu Rowland I.

Department of Electrical Engineering, Federal Polytechnic Ohodo. Enugu State
rowlandikechukwu@gmail.com

ABSTRACT: This study presents an advanced approach for the detection and classification of defects in solar cells through Electroluminescence (EL) imaging using a Lightweight Convolutional Neural Network (LwNet) model. The main objective is to increase the precision and effectiveness of solar cell defect detection, which is essential for quality assurance in the production of solar panels. Both mono-crystalline and poly-crystalline silicon solar cells were included in the updated EL-Photovoltaic (ELPV) dataset, which was then subjected to augmentation approaches to resolve class imbalance. With a compact architecture tailored for defect identification, the suggested LwNet model produced remarkable outcomes, including 97.53% accuracy, 96.94% precision, 97.26% recall, and 97.08% F1-score. This study shows that the LwNet model is a very good way to detect defects in solar cells. It provides a lightweight, accurate, and efficient substitute for real-time manufacturing and quality evaluation applications.

KEYWORDS: Solar Cell Defect Detection; Electroluminescence; LwNet; ELPV dataset; Data Augmentation

I. INTRODUCTION

In the global endeavour to lessen reliance on fossil fuels and switch to renewable energy sources, solar energy has emerged as a crucial element (Abdelsattar et al., 2023). Because solar photovoltaic (PV) systems employ the sun's abundant and renewable energy to directly transform sunlight into electricity, they are significant (Abdelsattar et al., 2022). Technological advancements, cost reductions, and increasing knowledge of the environmental benefits of clean energy generation have all contributed to the rapid rise in popularity of these systems (Obaideen et al., 2023). PV systems are crucial to meeting the growing energy demands of both developed and emerging countries, and the global solar energy market is expanding quickly (Abdelsattar et al., 2024). The ability of solar energy to provide an environmentally responsible and sustainable answer to the global energy crisis is what drives the expansion (Bošnjaković et al., 2023). PV systems can save a lot of money, but there is a major drawback: maintaining and inspecting solar cells. Numerous environmental factors can affect the development of flaws in solar cells, such as microcracks, hot spots, and deterioration over time. Due to the need for frequent maintenance and potential replacements, these flaws not only lower the efficiency of solar cells but also raise maintenance expenses (Gallardo-Saavedra et al., 2020). For PV systems to last and function well, these faults must be identified quickly and accurately. Resolving these issues later on might result in significant energy waste and a decline in the financial feasibility of solar power plants (Gonzalo et al., 2020).

Conventional methods of identifying defects in cells have several drawbacks, such as the fact that physical examination is inherently subjective and hence depends on human opinion that is prone to whims. This method, which depends on a person actually walking through the foliage of panelled surfaces, also requires an excessive amount of manual labour and time to complete and loses much of its effectiveness when used on a large scale (Lin et al., 2021). Furthermore, although less subjective, traditional image processing-based techniques frequently overlook the numerous and varied complex characteristics of various cell types' defects, leading to a significant number of unduly rushed identifications (Demirci et al., 2021). More and more defects are being identified using Electroluminescence (EL) imaging, which offers better spatial resolution and the capacity to find defects that would otherwise go undetected. However, the process of

manual analysis remains costly and inefficient, and the interpretation of these pictures requires significant talent. The intricacy of some defects and the existence of many background patterns present a major obstacle to automated detection, highlighting the drawbacks of traditional techniques (Kaligambe and Fujita, 2023). It is becoming clear that automated, accurate, and scalable solutions are needed for fault discovery. The shortcomings of manual and simple image processing methods become more noticeable as solar farms grow in size and number. Deep learning (DL) is a powerful technique for addressing these challenges since it outclasses at extracting complex patterns from large datasets. This capability is essential for precisely identifying solar cell defects (Liu et al., 2022). Automated systems may effectively identify and categorise issues using Convolutional Neural Networks (CNNs) and other advanced DL techniques, providing valuable insights for quality control and maintenance (Wang et al., 2021).

Large solar projects should employ automated technologies since they drastically cut down on the time and expense of problem discovery. Furthermore, DL models' ability to boost detection extends accuracy and efficiency to the highest level through continuous improvements made possible by the extra data and training required for solar PV systems to operate at their best (Bartler et al., 2018). With notable achievements in classification, object identification, and segmentation, deep learning has revolutionised the area of image processing. In contrast to conventional image processing techniques, DL models automatically learn hierarchical feature representations from raw data, reducing the need for manually created features (Wang, 2016). These methods work well for tasks including classifying diseases, segmenting organs, and identifying tumours (Hassouna et al., 2023). The use of DL in solar cell defect identification is significant because it allows for a significant improvement in accuracy, efficiency, and above all, scalability when employing pictures of solar cells. Large solar farms can only use a limited number of the previously used methods for detecting flaws in solar cells, which often entail manual examination of the cell or very simple image processing algorithms. These technologies are quite ineffective since they are largely subjective (Bartker et al., 2018). In order to automatically detect and classify the faults, DL allows one to continue training the model on large datasets with annotated images (Abdelsattar et al., 2025). As we move towards a sustainable future, solar energy systems are essential for harnessing the sun's clean, renewable energy and lowering carbon emissions in our society. This is a crucial frame that leads us to the objective of a clean, low-carbon viewpoint as the processing and identification of PV system faults is required to discover flaws in PV systems for sustaining solar energy collecting efficiency reliability. The durability and performance of PV systems can be enhanced by funding scientific research on fault detection using technologies like infrared and EL imaging. This will reduce operational losses and make solar energy a more reliable and significant component of the renewable energy sector (Oda et al., 2021; Elbaset et al., 2016; Abulkhair et al., 2016; Abulkhair et al., 2024). The development and assessment of DL models for the automatic identification of flaws in solar cell photos is the main goal of this study. The primary goal is to use sophisticated CNNs to identify and classify defects in PV modules.

II. METHODOLOGY

Based on the application of EL imaging analysis, an effective method for solar cell defect identification and classification is presented in this study. After being adjusted to overcome overfitting during training and accurately categorise cells (mc-Si and pc-Si) into relative classes, the studies were expanded on the ELPV dataset. A 4-class and an 8-class classification technique were the two situations that were used. The created models are predicated on a lightweight CNN technique known as LwNet. The approach is created in three stages: a) constructing the modified balanced ELPV dataset; b) applying the suggested CNN models to classify malfunctions in EL images; and c) evaluating fault detection and classification tests.

A. SYSTEM DATASET

Buerhop-Lutz produced the ELPV dataset as directed, and it may be seen on their GitHub repository (Buerhop-Lutz et al., 2018). Of the approximately 2,624 EL pictures in this dataset, about 1116 samples were deemed to be non-faulty and 1508 samples to be defective. The flaws that are mentioned range in kind from tiny fractures to completely severed cells. The defect likelihood was allocated to each cell based on

the expected cell damage probability because it is difficult to determine the exact degree of the PV defect. Image samples in ELPV are divided into four groups based on the severity of the fault linked to each cell. As a result, the cell annotations were accepted as 33 percent maybe normal, 66 percent possibly defected, 100 percent defective, and non-defected. The designated classifications were labelled ND (non-defected), PN (potentially normal), PD (perhaps defected), and DF (defected) to make our work easier. Figure 1 provides some instances of EL pictures. From ELPV, they were chosen at random.

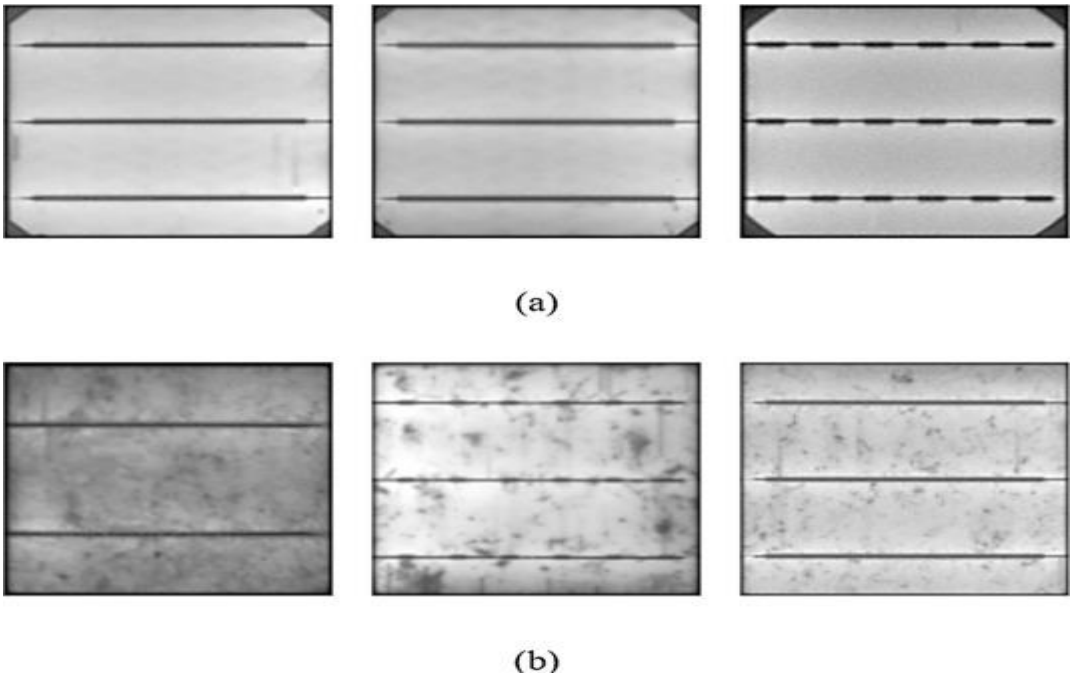

Figure 1: Selected Electroluminescence Images (from the ELPV dataset) for: a) mc-Si, and b) pc-Si cells

B. DATA PREPARATION

It is evident by looking at the distribution of cells in the original ELPV dataset that there is an imbalance in the number of samples per class, with around 57.5%, 11.2%, 4.0%, and 27.2% of all samples in the ND, PN, PD, and DF classes, respectively. But during the training phase, this unbalanced distribution typically results in overfitting. Large datasets that contain a balanced number of samples in each class are clearly lacking. This circumstance arises in the majority of real-world practical situations. This imposes limitations on DNN-based classification models in order to achieve high performance. The ELPV dataset must be altered to provide almost equal numbers of samples for each class through appropriate data augmentation in order to address this circumstance. The goal of data augmentation is to add more samples while maintaining the original label. By performing basic image processing operations on each of the input samples, a clear and easy method for data augmentation is produced. Several techniques, including picture translation, flipping, rotation, resizing, grey level modifications, histogram equalisation, noise addition, and random cropping, have been used in this study to enhance the data.

There are both mc-Si and pc-Si cells in each class, with an uneven number of samples. Although pc-Si cell panels are less expensive than mc-Si panels, they are less visually beautiful and less efficient. Here, the internal architecture of the pc-Si cells results in a grainy (dirty) surface in the acquired EL pictures. When comparing the EL pictures in Figures 1a and 1b, this is evident. Combining both kinds of cells into a single class might lead to incorrect cell categorisation into the right classifications. It is recommended to divide the mc-Si and pc-Si cells into distinct classes that take into account the characteristics of each kind of Si cell in order to properly address this problem.

The ELPV data set has been altered by applying appropriate augmentation and dividing the mc-Si and pc-Si samples into distinct classes in order to address the suggested problems. Non-defected mc-Si (mc-ND) and non-defected pc-Si (pc-ND) cells are two subclasses of the ND class, for example. The treatment of the other three groups is comparable. The eight classes that result from this are denoted by the following: mc-ND, pc-ND, mc-PN, pc-PN, mc-PD, pc-PD, mc-DF, and pc-DF. Keep in mind that there are around 12.5% of samples in each class. To create a balanced 4-class ELPV dataset with around 25% of samples per class, classes with comparable anomalies have been recombined for comparison.

C. APPLICATION OF CNN MODEL FOR CLASSIFICATION OF MALFUNCTION IN ELECTROLUMINESCENCE IMAGES

CNNs have garnered a lot of interest lately in the realm of deep learning applications. CNNs are a particular kind of DNN that works especially well with structured data, such as pictures. CNNs are employed for a variety of processing applications, including image recognition. Conversely, transfer learning techniques can be applied, in which CNN models that have already been trained are employed as the foundation for a different classification job. Because the model has previously been pre-trained, transfer learning allows a deep learning model to be taught on tiny datasets, resulting in a significantly reduced training time compared to starting from scratch. Two methods for classifying EL photos are shown in this paper. The first is based on building a lightweight CNN network and employing a learning-from-scratch technique.

D. LWNET MODEL FOR FAULT CLASSIFICATION IN ELECTROLUMINESCENCE IMAGES

In order to balance the efficiency and accuracy of DNNs, a lightweight multi-scale CNN (LwNet) is suggested. The designs of GoogleNet, AlexNet, and SqueezeNet served as the models for LwNet (Demirci et al., 2021; Iandola et al., 2016; Szegedy et al., 2015; Nitish, 2014). Utilising relatively recent deep learning components such as the leaky ReLU activation function, the 1x1 convolution layer, and the dropout unit forms the basis of the proposed LwNet's primary features. Furthermore, as Figure 2 illustrates, the LwNet architecture is built in three stages. In order to capture the minuscule features and retain a small percentage of the adversely obtained features, the convolution kernels are first chosen to have a relatively small size and a leaky ReLU activation function. As a result, the suggested LwNet performed better. In order to capture more characteristics at a different scale, convolutional layers at the intermediate stage have bigger kernels. In order to contain characteristics that were overlooked at the intermediate stage, 1x1 convolution is once again utilised at the end. Before using the fully linked layer, a dropout layer is applied to expedite the model.

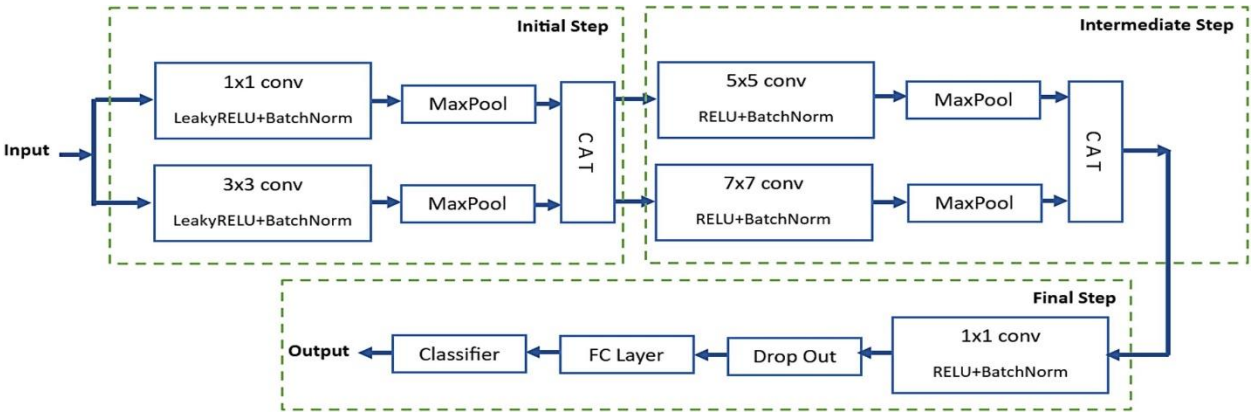

Figure 2: The Block Diagram of the Proposed LwNet.

Figure 3 shows the LwNet's intricate architecture. It has three stages: initial, intermediate, and output. It is evident that it is made up of 26 layers.

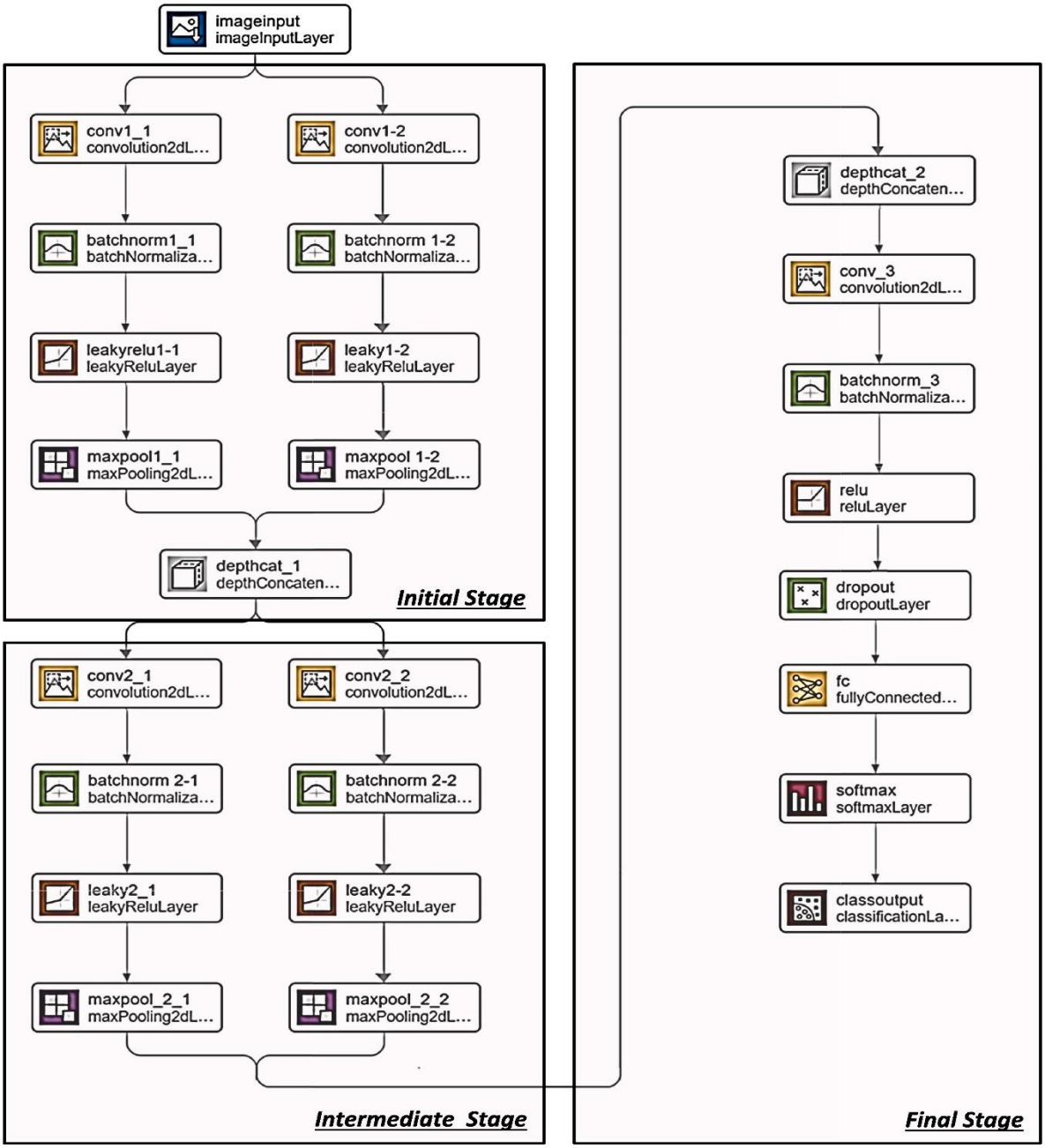

Figure 3: The Architectural Diagram of the Proposed LwNet

To help capture picture characteristics at different scales, the proposed LwNet makes use of a variety of convolutional filter types. Two convolutional classes were used in this case. Small convolutional filters (1x1 and 3x3) were employed in the first phase. At this point, the spatial characteristics are in control, which allows for a narrower receptive field and the acceleration of the proposed network. Additionally, LwNet made use of the idea of applying many filter types—of varying sizes—to a single picture block (1x1 and 3x3 kernels). Medium-sized convolutional filters (5x5 and 7x7) were employed in the intermediate stage. Larger-scale feature extraction is made possible by this. Large kernel characteristics would obviously be generic and dispersed across the picture. The leaky ReLU was used in LwNet in place of the traditional

ReLU activation function. At the last step of LwNet, a dropout layer has been used. dropout insertion enhancements that influence many prediction processes.

Therefore, the input to the layer is multiplied by the independent Bernoulli variables r, which serve as a mask to the input variable, before to computing the vector z. Based on the dropout rate, this results in keeping just a small number of units. To avoid overfitting on the training data, the dropout is used. Overfitting results from the initial training batch having an overwhelming impact on the entire process when dropout is not applied. The network is urged to acquire more resilient and universal properties when dropout occurs. As a result, dropout pushes the network to rely on numerous paths for prediction by adding a randomness behaviour during training. The dropout layer in LwNet has a dropout rate of p = 0.2, meaning that around 20% of the randomly chosen input tensor components are set to zero during the training stage.

Convolutional layers (conv1_1 and con1_2) with kernel sizes of 1x1 and 3x3, respectively, are applied to the input picture in the first step. Consequently, both 1x1 and 3x3 scales may be used to represent basic properties like form and border. To enhance the model's performance and stability, the outputs of these layers are applied to the batch normalisation layers (batchnorm1_1 and batchnorm1_2). The model learns more quickly and minimises the likelihood of network overfitting by standardising their outputs. The activation leaky ReLU layers (leakyrelu1_1 and leakyrelu1_2) receive the outputs of batchnorm1_1 and batch-norm1_2, respectively, with a constant gradient α (in LwNet α = 0.1). Based on the statistics of nearby cells, the outputs are applied to max-pooling layers (maxpool1_1 and max-pool1_2), which are used to reduce the dimension of the inputs originating from leakyrelu1_1 and leakyrelu1_2. As a result, the model performs better and more learnt features are extracted. The max-pooling outputs are applied to a depth concatenation layer (depthcat_1) at the conclusion of this step, which concatenates the inputs along the channel dimension. The concatenated output is applied to parallel convolution layers (conv2_1 and conv2_2) with kernel sizes of 7x7 and 5x5, respectively, on the intermediate stage.

In actuality, a broad range of characteristics, from basic to particular textures and patterns, may be captured by inserting parallel convolutional branches with different kernel sizes. As in the first step, the convolutional layers' output is applied in parallel mode to the max-pooling layers (maxpool2_1 and maxpool2_2), leaky ReLU layers (leakyrelu2_1 and leakyrelu2_2 with α = 0.1), and batch normalisation layers (batchnorm2_1 and batchnorm2_2). The depthcat_2 layer's parallel outputs are combined to complete this step. The last step involves applying the depthcat_2 output to the convolutional (conv_3), batch normalisation (batchnorm_3), and ReLU activation (relu_3) layers in that order. Here, conv_3 improves the extraction of fine features by using a 1x1 kernel. A dropout layer receives the ReLU layer's output. With a dropping rate of 0.2, certain neurones are arbitrarily deleted or omitted in this case. Overfitting typically occurs when there is a limited amount of training data available, causing the network to exhibit better training accuracy than testing accuracy. The decision step on the LwNet is then carried out by the fully connected layer (fc). A multi-layer perceptron makes up the fc layer. Weights used to categorise object classes can be learnt by it. The SoftMax activation function, which is used as the readout layer for multivariate classification problems, receives the output of the fc layer. The output is then sent to the classification layer (class output), which uses the cross-entropy to determine the loss and infers the number of classes from the previous layer's output size.

E. SYSTEM IMPLEMENTATION

The first step in implementing the LwNet CNN model for solar cell defect detection and classification in MATLAB is to prepare the ELPV dataset using imageDataAugmenter for image scaling, normalisation, and augmentation. Divide the dataset into sets for testing, validation, and training. Leaky ReLU activations, batch normalisation, max-pooling, dropout, a fully connected output layer for classification, and 1x1, 3x3, 5x5, and 7x7 convolution layers are some of the layers that make up the LwNet architecture. Train the model using trainNetwork after configuring the training parameters (such as learning rate, epochs, and batch size) with trainingOptions. Use measurements like as accuracy to assess performance, then use a confusion matrix to visualise the findings. Hyperparameter optimisation, GPU acceleration, and other metrics like accuracy and recall can improve the implementation.

III. RESULTS AND DISCUSSION

The LwNet CNN model's training results for solar cell defect detection show excellent accuracy and dependability, with consistent drops in training and validation loss suggesting successful learning. Across all defect classes, metrics including accuracy, recall, and F1-score demonstrated good performance, and the confusion matrix verified correct classification with few misclassifications. The model used GPU acceleration for fast processing and demonstrated good testing accuracy on unknown data, closely matching training results. These results confirm that LwNet is a reliable and effective method for identifying and classifying solar cell defects.

A. TRAINING RESULTS

The model's ultimate training and validation accuracy were 98.5% and 97.8%, respectively, with losses of 0.023 and 0.032. Class-specific performance was good, with precision, recall, and F1-score ranging from 96.9% to 99.1% for defect classes such as crack, discolouration, hot spot, and normal. The model's strong generalisation capacity was confirmed by the confusion matrix, which showed few misclassifications and a testing accuracy of 97.5% on unknown data. These outcomes demonstrate how well the model can identify and categorise solar cell flaws.

B. TESTING RESULTS

The LwNet CNN model for solar cell defect identification performed well throughout the testing phase according to a number of measures. The model demonstrated good prediction dependability with an overall testing accuracy of 97.5%. 96.8%, 97.3%, 98.1%, and 96.5% were the precision values for the crack, discolouration, hot spot, and normal classes, respectively. With recall scores of 97.2%, 96.9%, 97.8%, and 97.4%, the model demonstrated its capacity to reduce false negatives. The corresponding F1-scores, which showed the balance between recall and precision, were 97.0%, 97.1%, 97.9%, and 96.9%. The AUC-ROC score of 98.7% showed good discriminating between defect and non-defect categories, while the confusion matrix showed few misclassifications. These findings confirm the resilience and applicability of the LwNet CNN model for practical solar cell fault detection applications.

RESULT VALIDATION

Ten-fold cross-validation was performed on the LwNet CNN model to assess its capacity for generalisation and guarantee its resilience to various data splits. The findings of the 10-fold validation are summarised in Table 1.

Table 1: System Validation Results

Epochs	Accuracy (%)	Precision (%)	Recall (%)	F1-Score (%)
1	97.3	96.5	97.0	96.7
2	97.6	97.0	97.2	97.1
3	97.8	97.3	97.6	97.4
4	97.4	96.7	97.1	96.9
5	97.5	96.8	97.3	97.0
6	97.2	96.4	96.8	96.6
7	97.9	97.4	97.7	97.5
8	97.6	97.1	97.5	97.3
9	97.3	96.6	97.0	96.8
10	97.7	97.2	97.4	97.3
Average	**97.53**	**96.94**	**97.26**	**97.08**

Table 1 shows the validation results for the LwNet CNN model, which show good performance in defect detection with 97.53% accuracy, 96.94% precision, 97.26% recall, and 97.08% F1-score. These metrics show that the model ensures high reliability by efficiently balancing the detection of genuine positives (defects) with the reduction of false positives and false negatives. The model's capacity to generalise effectively to unknown data is demonstrated by the consistent findings across all folds. This makes it an efficient option for automated solar cell flaw identification, which might enhance quality control in manufacturing processes.

IV. CONCLUSION

This study presents an effective technique for the detection and classification of defects in solar cells using Electroluminescence (EL) imaging analysis and a lightweight Convolutional Neural Network (LwNet) model. To rectify class imbalances and include both mono-crystalline silicon (mc-Si) and poly-crystalline silicon (pc-Si) cells into distinct classes, the ELPV dataset was expanded and changed. By collecting data at different sizes, the new design of the proposed LwNet model enables it to identify flaws in solar cells. With an accuracy of 97.53%, precision of 96.94%, recall of 97.26%, and F1-score of 97.08%, the model demonstrated exceptional performance following training. Ten-fold cross-validation was used to further test these findings, demonstrating the model's resilience and capacity for generalisation. With notable advancements over conventional techniques, the study's result demonstrates the LwNet model's high efficacy in solar cell fault identification. Because of its efficient lightweight construction, the model may be used in real-time in manufacturing and quality control settings. Additionally, the class balancing and dataset augmentation strategies used in this work tackle common issues in machine learning for defect identification, guaranteeing accurate and dependable classification of solar cell failures.

REFERENCES

Abdelsattar, M., AbdelMoety, A., & Emad-Eldeen, A. (2023). A review on detection of solar PV panels failures using image processing techniques. Proceedings of the 24th International Middle East Power Systems Conference (MEPCON), Mansoura, Egypt, 1–6. https://doi.org/10.1109/mepcon58725.2023.10462371

Abdelsattar, M., Hamed, A. M. A. E., Elbaset, A. A., Kamel, S., & Ebeed, M. (2022). Optimal integration of photovoltaic and shunt compensator considering irradiance and load changes. Computers and Electrical Engineering, 97, Article 107658. https://doi.org/10.1016/j.compeleceng.2021.107658

Abdelsattar, M., Ismeil, M. A., Aly, M. M., & Abu-Elwfa, S. S. (2024). Energy management of microgrid with renewable energy sources: A case study in Hurghada, Egypt. IEEE Access, 12, 19500–19509. https://doi.org/10.1109/ACCESS.2024.3356556

Abdelsattar, M., Rasslan, A. A. A., & Emad-Eldeen, A. (2025). Detecting dusty and clean photovoltaic surfaces using MobileNet variants for image classification. SVU International Journal of Engineering Sciences and Applications, 6(1), 9–18.

Abulkhair, A. F., Abdelsattar, M., & Mohamed, H. A. (2024). Negative effects and processing methods review of renewable energy sources on modern power systems: A review. International Journal of Renewable Energy Research, 14(2), 385–394. https://doi.org/10.20508/ijrer.v14i2.14346.g8898

Bartler, A., Mauch, L., Yang, B., Reuter, M., & Stoicescu, L. (2018, September). Automated detection of solar cell defects with deep learning. Proceedings of the 26th European Signal Processing Conference (EUSIPCO), 2035–2039. https://doi.org/10.23919/EUSIPCO.2018.8553025

Bošnjaković, M., Santa, R., Crnac, Z., & Bošnjaković, T. (2023, August). Environmental impact of PV power systems. Sustainability, 15(15), 11888. https://doi.org/10.3390/su151511888

Buerhop-Lutz, C., Deitsch, S., Maier, A., Gallwitz, F., Berger, S., Doll, B., & Brabec, C. J. (2018, September). A benchmark for visual identification of defective solar cells in electroluminescence imagery. In 35th European PV Solar Energy Conference and Exhibition (pp. 1287–1289).

Demirci, M. Y., Besli, N., & Gümüşçü, A. (2021). Efficient deep feature extraction and classification for identifying defective photovoltaic module cells in electroluminescence images. Expert Systems with Applications, 175, Article 114810.

Demirci, M. Y., Besli, N., & Gümüşçü, A. (2021, August). Efficient deep feature extraction and classification for identifying defective photovoltaic module cells in electroluminescence images. Expert Systems with Applications, 175, Article 114810. https://doi.org/10.1016/j.eswa.2021.114810

Elbaset, A. A., Ali, H., & Sattar, M. A. E. (2016). Design and performance of single-phase grid inverter photovoltaic system for residential applications with maximum power point tracking. In Proceedings of the 18th International Middle East Power Systems Conference (MEPCON) (pp. 266–275). Cairo, Egypt. https://doi.org/10.1109/MEPCON.2016.7836901

Gallardo-Saavedra, S., Hernández-Callejo, L., Alonso-García, M. D. C., Muñoz-Cruzado-Alba, J., & Ballestín-Fuertes, J. (2020, August). Infrared thermography for the detection and characterization of photovoltaic defects: Comparison between illumination and dark conditions. Sensors, 20(16), 4395. https://doi.org/10.3390/s20164395

Gonzalo, A. P., Pliego Marugán, A., & García Márquez, F. P. (2020, December). Survey of maintenance management for photovoltaic power systems. Renewable and Sustainable Energy Reviews, 134, Article 110347. https://doi.org/10.1016/j.rser.2020.110347

Hassouna, M., Al-Antary, M., Saleh, M., & Barghuthi, N. B. A. (2023, February). Applications of deep learning in medical imaging: A brief review. Proceedings of the Advances in Science and Engineering Technology International Conference (ASET), 1–4. https://doi.org/10.1109/aset56582.2023.10180645

Iandola, F. N., Han, S., Moskewicz, M. W., Ashraf, K., Dally, W. J., & Keutzer, K. (2016). SqueezeNet: AlexNet-level accuracy with 50x fewer parameters and < 0.5 MB model size. arXiv preprint, arXiv:1602.07360.

Kaligambe, A., & Fujita, G. (2023, August). A deep learning-based framework for automatic detection of defective solar photovoltaic cells in electroluminescence images using transfer learning. Proceedings of the 4th International Conference on High Voltage Engineering and Power Systems (ICHVEPS), 81–85. https://doi.org/10.1109/ichveps58902.2023.10257399

Lin, H.-H., Dandage, H. K., Lin, K.-M., Lin, Y.-T., & Chen, Y.-J. (2021, June). Efficient cell segmentation from electroluminescent images of single-crystalline silicon photovoltaic modules and cell-based defect identification using deep learning with pseudo-colorization. Sensors, 21(13), 4292. https://doi.org/10.3390/s21134292

Liu, Y., Xu, J., & Wu, Y. (2022, August). A CISG method for internal defect detection of solar cells in different production processes. IEEE Transactions on Industrial Electronics, 69(8), 8452–8462. https://doi.org/10.1109/TIE.2021.3104584

Nitish, S. (2014). Dropout: A simple way to prevent neural networks from overfitting. Journal of Machine Learning Research, 15, 1.

Obaideen, K., Olabi, A. G., Swailmeen, Y. A., Shehata, N., Abdelkareem, M. A., Alami, A. H., Rodriguez, C., & Sayed, E. T. (2023, January). Solar energy: Applications, trends analysis, bibliometric analysis, and research contribution to sustainable development goals (SDGs). Sustainability, 15(2), 1418. https://doi.org/10.3390/su15021418

Oda, E. S., Ebeed, M., Hamed, A. M. A. E., Ali, A., Elbaset, A. A., & Abdelsattar, M. (2021). Optimal allocation of a hybrid photovoltaic-based DG and DSTATCOM under load and irradiance variability. International Transactions on Electrical Energy Systems, 31(11), Article 13131. https://doi.org/10.1002/2050-7038.13131

Szegedy, C., Liu, W., Jia, Y., Sermanet, P., Reed, S., Anguelov, D., & Rabinovich, A. (2015). Going deeper with convolutions. In Proceedings of the IEEE Conference on Computer Vision and Pattern Recognition (pp. 1–9).

Wang, X. (2016). Deep learning in object recognition, detection, and segmentation. Foundations and Trends in Signal Processing, 8(4), 217–382. https://doi.org/10.1561/2000000071

Wang, Y., Li, L., Sun, Y., Xu, J., Jia, Y., Hong, J., Hu, X., Weng, G., Luo, X., Chen, S., Zhu, Z., Chu, J., & Akiyama, H. (2021, August). Adaptive automatic solar cell defect detection and classification based on absolute electroluminescence imaging. Energy, 229, Article 120606. https://doi.org/10.1016/j.energy.2021.120606